ミストデポジションと高水分散性 ITO ナノ粒子によるフレキシブル基板上への高性能 ITO 薄膜の作製

鈴木涼子，西　康孝，松原正樹，村松淳司，蟹江澄志

Fabrication of High-Performance ITO Flexible Thin Films Utilizing Mist Deposition and ITO Nanoparticles with High Water Dispersibility[†]

Ryoko SUZUKI, Yasutaka NISHI, Masaki MATSUBARA, Atsushi MURAMATSU and Kiyoshi KANIE

フレキシブルデバイスの作製において，耐熱性の乏しい樹脂基板への透明導電膜の低温成膜は重要な技術である．ミストデポジションは超音波振動子を用いて霧化させた原料を基板に吹き付けて成膜する手法である．高温処理が不要であることから樹脂基板への成膜に適した手法だと考えられる．本報告ではミストデポジションと以前我々が報告した高水分散性酸化インジウムスズ（ITO）ナノ粒子を組み合わせて透明導電膜の作製を試みた．ミストデポジションで作製した ITO ナノ粒子膜は他の成膜法で成膜した場合よりも低い表面粗さと低い抵抗率を示した．成膜条件の制御が容易なミストデポジションを用いることで膜内部，表面での ITO ナノ粒子の凝集を抑制する条件の調整が可能であり，高性能透明導電膜の作製が可能であることが分かった．

In process of preparation of flexible device, providing a low-temperature coating method of transparent conductive film for polymeric a substrate with low heat tolerance is very important. Mist deposition is a suitable method for coating these substrates as high-temperature processes are not required. Herein, mist is formed by atomizing the coating liquid. Subsequently, it is deposited on the substrate and dried to form a thin film. In this report, a transparent conductive film is prepared utilizing mist deposition and indium tin oxide (ITO) nanoparticles with high water dispersibility, as detailed in our previous report. The mist-deposited ITO thin film exhibits the lowest roughness and resistivity when compared to the films formed using other coating methods. The results indicate that a densely packed film can be prepared by changing the coating conditions, which are easily controlled during the mist deposition. Thus, a high-performance transparent conductive film is successfully prepared using an "eco-friendly" process without high-temperature treatment.

Key words　ミストデポジション法，ITO ナノ粒子，透明導電膜
mist deposition method, ITO nanoparticles, transparent conductive film

1　Introduction

Recently, low-temperature processes for the fabrication of electric wiring on substrates with poor heat tolerances have become important technologies owing to the growth of flexible devices [1] and film-type solar cells [2]. In particular, printed electronics (PE), which is the direct drawing of electrical wirings onto a substrate using conventional printing methods [3]–[5], is one of the most attractive technologies. Resist coating, exposure, and etching, which are included in the conventional process for fabrication of the electrode, are not necessary in the PE process. Therefore, PE has the advantages of low environmental load and low cost. However, the drawing of electrical wiring requires the use of conductive pastes, which results in a higher resistivity of PE electric wirings than that of the conventional process.

Indium tin oxide (ITO) is a transparent conductive oxide with low resistivity, high transparency, and moderate chemical stability and is the most commonly used material for transparent electrodes [6]. Transparent conductive films

using ITO nanoparticles have been prepared by inkjet-printing [7]–[9] and brash printing [10], [11]. In these reports, organic solvents and dispersants were used for the preparation of ink containing ITO nanoparticles; therefore, high-temperature treatment (possibly over 400°C) was necessary to remove organic residue for the preparation of low-resistivity ITO electric wiring. Essentially, only substrates with heat resistance can be used in the PE process.

Mist deposition, which does not use organic solvents and dispersants, has been reported as a method for the fabrication of films consisting of nanoparticles. The mist deposition process is as follows. First, the coating liquid is atomized. The resulting mist is carried by a carrier gas, deposited on the substrate, and dried to form films (Fig. 1a). The mist deposition method is similar to that of spray coating; however, the droplets in the mist are smaller than those in spray coating and remain in the air for a longer period. From this characteristic, mist deposition has the advantages of mist droplet transportation by a carrier gas and control of the film structure by tuning the gas flow. Among the reports on mist deposition, there are several reports on mist chemical vapor deposition (CVD) [12]–[14]. Gallium-doped ZnO (GZO) film and boron-doped ZnO (BZO) film were prepared by mist CVD. On the other hand, there are a few reports on mist deposition using nanoparticles. Qin *et al*. prepared a mist-deposited TiO_2 nanoparticle film [15] where a TiO_2 nanoparticles aqueous dispersion was used as the coating liquid and deposited on a Si wafer heated to 150°C. The obtained films exhibited a characteristic ring pattern on their surfaces. These patterns were formed by the aggregation of TiO_2 nanoparticles during the evaporation of water from the mist droplets on the substrate. Additionally, these patterns differed according to their position inside the Si wafer. These results indicated that mist deposition can be used to fabricate films using a low-temperature process and the surface structure of the film can be controlled by changing the evaporation conditions.

In our previous reports, protruded ITO nanoparticles [16] had a much higher water dispersibility than conventional cubic-shaped ITO nanoparticles [17]. The protruded ITO nanoparticles were single-crystalline nanoparticles with many protrusions on their surfaces, which resulted in a larger surface area and higher surface water absorption than cubic-shaped ITO nanoparticles. These protruded ITO nanoparticles could maintain their dispersion state in an aqueous medium for over one month without any dispersant. Hence, protruded ITO nanoparticles can be applied for mist deposition because of their high water dispersibility. Therefore, we expect that protruded ITO nanoparticles can form densely packed and flat surfaced films using mist deposition during a low-temperature process.

Herein, we report the advantages of mist deposition for the fabrication of transparent conductive films and the advantages of using protruded ITO nanoparticles for mist deposition.

2 Experimental Procedure

ITO nanoparticles were prepared as described in our previous reports [16], [17]. Two types of ITO nanoparticles, C-NP and P-NP, were prepared, which were cubic-shaped and protruded ITO nanoparticles, respectively, with an Sn doping of 14 at%. C-NP and P-NP powders were added to water and dispersed using a homogenizer to prepare an aqueous dispersion of ITO nanoparticles. P-NP had a higher water dispersibility in water than C-NP because of the high hydrophilicity originated from its shape. P-NP maintained a good dispersibility for over one month; whereas, C-NP settled at the bottom of the vessel after standing for one day.

ITO thin films on the substrates were prepared using the mist deposition system (Fig. 1b, 1c). The mist generation unit consisted of four ultrasonic oscillator units. The mist produced from ITO nanoparticle aqueous dispersion was transported by an N_2 carrier gas and deposited on the substrate. On the way, it was passed through a water trap to remove large mist droplets. The flow rate was fixed at 10–20 L·min^{-1} and the resulting thin films were heat treated in air. The thickness of the ITO thin films was adjusted to 300 nm by controlling the deposition period.
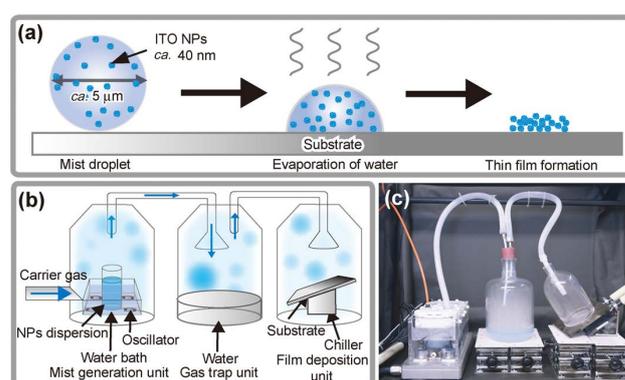

Fig. 1　(a) Scheme of film formation by mist deposition, (b) scheme of mist deposition system, and (c) appearance of experimental mist deposition system.

3 Results and Discussion

3.1. Preparation of C-NP and P-NP

From X-ray diffraction (XRD) measurement, it was confirmed that C-NP and P-NP had In_2O_3 crystal structure

(JCPDS No. 6–0416). Then, the doping amounts of Sn based on In calculated from the inductively coupled plasma (ICP) results were 14.4 mol% and 14.2 mol% in C-NP and P-NP, respectively. From these results, it was confirmed that ITO was successfully prepared. Transmission electron microscopy (TEM) and high-resolution TEM (HR-TEM) images of C-NP and P-NP are shown in Fig. 2. C-NP had a cubic shape with smooth edge surfaces (Fig. 2a), whereas P-NP had a large number of protrusions on the surface (Fig. 2c). The mean particle size of C-NP and P-NP were 39 ± 12 and 38 ± 10 nm, respectively. In the HR-TEM images (Fig. 2b, 2d), C-NP and P-NP showed uniform crystal orientations. The crystallite sizes of C-NP and P-NP were calculated to be 35 and 33 nm, respectively, using Scherrer's equation. The calculated sizes were close to the mean particle diameters determined by TEM observations. The results suggested that C-NP and P-NP have single-crystalline structures. Additionally, the uniform distribution of In and Sn atoms in the nanoparticles was confirmed by energy-dispersive X-ray spectroscopy (EDS) mapping images. These results indicate the successful preparation of the two types of ITO nanoparticles.
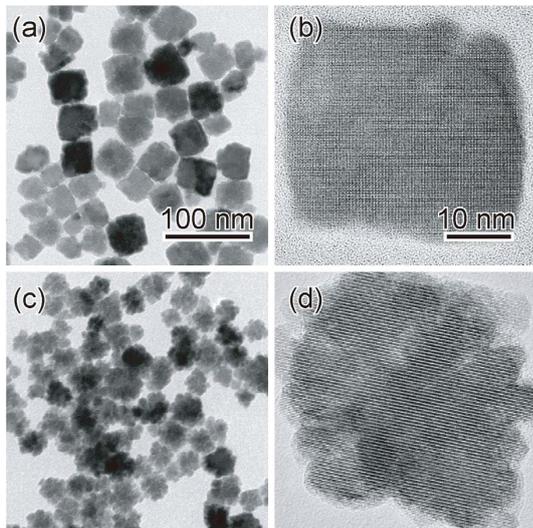

Fig. 2 Transmission electron microscopy (TEM) images of (a) C-NP and (c) P-NP, and high resolution (HR)-TEM images of (b) C-NP and (d) P-NP.

3.2. Effect of Deposition Method on Resistivity of P-NP Thin Films

To investigate the effect of the coating methods on resistivity, a glass substrate was coated with P-NP using several coating methods: mist deposition, bar coating, spray coating, spin coating, and drop casting. Fig. 3a shows the resistivities of P-NP thin films prepared by the different coating methods after heat treatment at 150, 200, 300, 400, and 500°C for 1 h

under an H_2-Ar (4% H_2) atmosphere.

The mist-deposited P-NP film had the lowest resistivity (9.0×10^{-3} Ω·cm) after heat treatment at 150°C. At the same process temperature, the resistivities of the films fabricated by bar-coating, spray coating, spin coating, and drop casting were 3.0×10^{-1} Ω·cm, 4.0×10^{-2} Ω·cm, 5.0×10^{-2} Ω·cm, and 4.0×10^{-2} Ω·cm, respectively. The resistivity of the thin films decreased with increasing process temperature for all coating methods. After heat treatment at 500°C, the mist-deposited films had the lowest resistivity 5.0×10^{-3} Ω·cm. Fig. 3b–3f show scanning electron microscopy (SEM) images of the surfaces of the P-NP films after heat treatment at 150°C. From the SEM images (Fig. 3b, 3c, 3e), it was observed that P-NP films prepared by the mist deposition, spray coating, and spin coating methods had flat and smooth surfaces. In contrast, the bar-coated (Fig. 3d) and drop-casted (Fig. 3f) P-NP films had rough surfaces with aggregated P-NP structures. The roughness (R_a) of the P-NP film surfaces was measured by atomic force microscopy (AFM). The mist-deposited P-NP films had the lowest R_a of 7.6 nm. Additionally, bar-coated, spray-coated, spin-coated, and drop-casted P-NP films exhibited an R_a of 7.8, 10.0, 15.8, and 12.6 nm, respectively. In a previous report [18], the resistivity of ITO thin film decreased with decreasing R_a. In this study, the P-NP film with the lowest R_a exhibited the lowest resistivity.

Above mentioned about mist deposition, the evaporation rate of liquids in the droplets can be adjusted by controlling the substrate temperature and carrier gas flow rate, which reduces the agglomeration of nanoparticles in the mist droplets and on the substrates. The insets of Fig. 3b–3f show
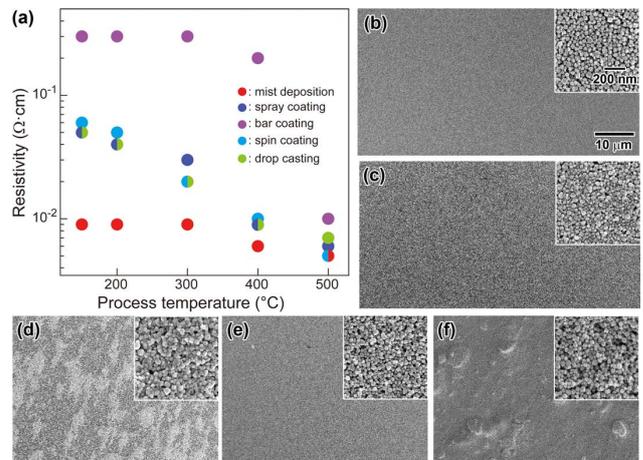

Fig. 3 (a) Resistivities of P-NP films prepared by different coating methods and scanning electron microscopy (SEM) images of P-NP film surface coated by (b) mist deposition, (c) spray coating, (d) bar coating, (e) spin coating, and (f) drop casting methods. These images were taken after annealing at 150°C. The insets in (b)-(f) are enlarged views of the surfaces.

enlarged views of the corresponding P-NP film surfaces. A densely packed uniform surface was observed, as shown in Fig. 3b, which indicates that mist deposition is advantageous for fabricating high-performance ITO thin films at low processing temperatures and is applicable to flexible films.

3.3. Characterization of Mist-Deposited C-NP and P-NP Films

ITO thin films were prepared by mist deposition using aqueous dispersions of C-NP and P-NP. Fig. 4a summarizes the resistivities of the C-NP and P-NP films fabricated by mist deposition in a low process temperature between room temperature and 200°C. Resistivities of the C-NP and P-NP films after annealing at 150°C were 8.0×10^{-2} Ω·cm and 9.0×10^{-3} Ω·cm, respectively. Fig. 4b–4c presents SEM images of the surfaces of the C-NP and P-NP films after annealing at 150°C, respectively. The C-NP film had a rough and porous surface structure. In contrast, a densely packed and flat surface was observed on the P-NP film. The lower resistivity of the P-NP film compared to that of the C-NP film can be attributed to the more densely packed structure of the P-NP film. Fig. 4d–4e present cross-sectional TEM images of C-NP and P-NP films on a polyethylene naphthalate (PEN) substrate (TEONEX, Q51–188, TOYOBO Co., Ltd., Osaka, Japan, t = 188 μm) with thicknesses of ca. 200 nm. These images correspond to the SEM images shown in Fig. 4b–4c. Loosely deposited porous inner structure with voids and irregularities was observed in the C-NP film. Additionally, a densely deposited inner structure of the P-NP film was observed. The difference in film structure between the C-NP and P-NP films is attributed to the difference in the dispersion states of C-NP and P-NP in the mist water droplets.
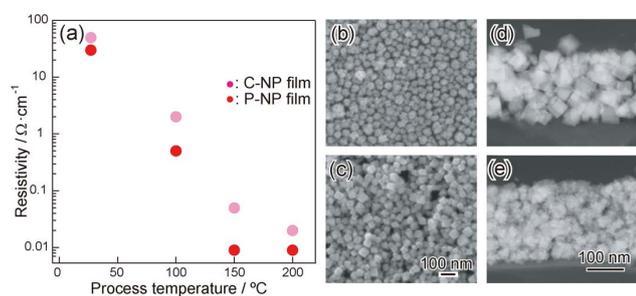

Fig. 4 (a) Resistivity of C-NP and P-NP films after heat treatment between room temperature and 200°C, scanning electron microscopy (SEM) images of the surfaces of the (b) C-NP and (c) P-NP films after annealing at 150°C, and cross-section transmission electron microscopy (TEM) images of (d) C-NP and (e) P-NP particles on polyethylene naphthalate (PEN) substrate.

The dispersion states of C-NP and P-NP in the mist water droplets were investigated using small-angle X-ray scattering (SAXS) measurements. In the water droplets, the mean particle size of particles in P-NP was 41 ± 13 nm, which was consistent with the size determined by TEM observation. This result indicates that P-NP were the primary particles in the water droplets. In contrast, C-NP had two particle sizes in water droplets, 54 ± 10 and 159 ± 30 nm. The smaller and larger sizes corresponded to the C-NP dispersed as primary and secondary particles, respectively. It was assumed that the high water dispersibility of P-NP resulted in a primary particle state in the water droplets. From these results, the stability of the ITO nanoparticles in aqueous dispersions was maintained in the mist water droplets and primary-dispersed nanoparticles can be used to form thin films with densely packed structures.

Furthermore, the effect of the ITO nanoparticle dispersion state was investigated. C-NP and P-NP films prepared using different elapsed times after the preparation of the aqueous dispersions were fabricated and their resistivities were measured (Fig. 5). The resistivity of the C-NP films increased as the elapsed time of the C-NP aqueous dispersion increased. Conversely, the P-NP films maintained a low resistivity regardless of the elapsed time. As mentioned in Section 2, C-NP has a lower water dispersibility than P-NP and settles at the bottom of the vessel after standing for one day. These results corresponded to the results that the high water dispersibility of P-NP was appropriate for high-performance ITO nanoparticle thin films.
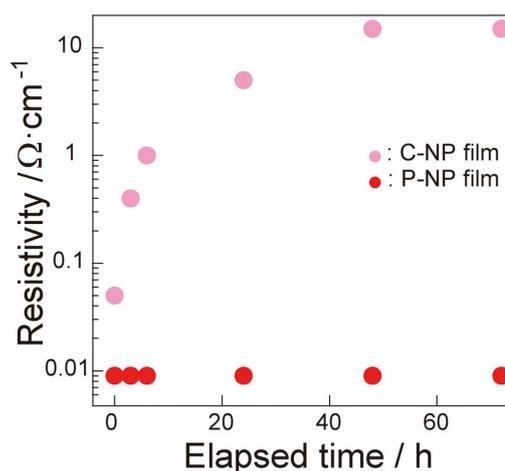

Fig. 5 Effect of elapsed time after preparation of indium tin oxide (ITO) nanoparticle dispersion on resistivity of mist-deposited film.

3.4. P-NP Mist Deposition on Flexible Films

P-NP was coated on a flexible PEN substrate by mist deposition with 300 nm thickness followed by annealing at 150°C for 1 h under N$_2$ atmosphere. The resulting P-NP film

showed high transparency (Fig. 6a) and had a low resistivity of 9.0×10^{-3} Ω ·cm, which is similar to the resistivity of P-NP film on a glass substrate. Additionally, the transmittance of this P-NP film was greater than 85% in the visible region (Fig. 6b). It was assumed that a highly transparent ITO thin film could be obtained on a flexible film by mist deposition. Furthermore, P-NP patterned films were fabricated by mist deposition on pre-treated hydrophilic flexible films. The method for selective deposition was as follows. First, Novec 1720 (3M) was precoated onto a PEN film (TEONEX, Q51−50, TOYOBO Co., Ltd., Osaka, Japan, t = 50 μm or t = 188 μm) to prepare a hydrophobic surface. The films were dried at 100℃ for 30 min. The films were masked using a patterned SUS430 thin substrate (t = 100 μm). The resulting masked PEN films were treated with a UV-ozone cleaner for 5 min to obtain patterned hydrophilic areas. Fig. 6c and Fig. 6d exhibit an SEM image and the corresponding EDS mapping image of the P-NP film In ions on a PEN substrate, respectively. The water droplets in the mist spontaneously were deposited on the hydrophilized area of the flexible films to form a uniform pattern. Selective and spontaneous processes will become a powerful technique for fabricating ITO-patterned films under ecofriendly atmospheric roll-to-roll PE conditions.
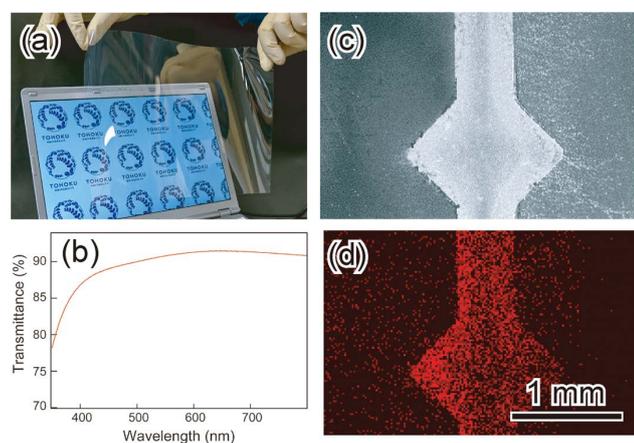

Fig. 6 (a) Appearance of P-NP film on polyethylene naphthalate (PEN) substrate coated by mist deposition, (b) transmittance spectra of the P-NP film, (c) scanning electron microscopy (SEM) image, and (d) corresponding energy-dispersive X-ray spectroscopy (EDS) mapping image of P-NP film In ions on patterned PEN substrate.

4 Conclusion

The design and synthesis of protruded ITO nanoparticles with high water dispersibility have been detailed in our previous report. ITO nanoparticles are one of the most stable materials for the fabrication of thin films using mist deposi-

tion. In this study, we prepared flexible films with high-performance ITO thin film on flexible film, that had low resistivity and high transparency using a combination of mist deposition and protrusion-rich ITO nanoparticles. A comparison to cubic ITO nanoparticles with low water dispersibility revealed that the high water dispersibility of protrusion-rich ITO nanoparticles played a critical role in fabricating high-performance ITO thin films. The high dispersibility of protrusion-rich ITO nanoparticles was maintained in mist water droplets. Protruded ITO nanoparticles were deposited on substrates in a primary particle state, and densely packed films were formed. The ITO thin films obtained by mist deposition have the following advantages. (i) Single-crystalline protrusion-rich ITO nanoparticles are readily dispersed in water for a long period without the use of surfactants or dispersants. (ii) ITO nanoparticle-based thin films can be fabricated under mild atmospheric conditions without the use of expensive vacuum production systems or dangerous and environmentally-harmful chemicals that are used in the current sputtering and etching procedure. Finally, (iii) Low resistivity and high transparency can be achieved with low-temperature annealing, which is applicable for the deposition of ITO thin films on flexible substrates. Mist deposition is a promising and powerful technique for the production of key materials essential for sustainable progress in PE technology as well as next-generation on-demand fabrication processes for wearable devices.

References

[1] J. Koo, D. Kim, H. Shim, T. Kim and D. Kim, "Flexible and Stretchable Smart Display: Materials, Fabrication, Device Design, and System Integration," *Adv. Funct. Mater.*, vol 28, no 35, pp. 1801834, 2018.

[2] Y. Li, G. Xu, C. Cui and Y. Li, "Flexible and Semitransparent Organic Solar Cells," *Adv. Ener. Mater.*, vol. 8, no 7, pp. 1701791, 2018.

[3] Y. Kamikoriyama, H. Imamura, A. Muramatsu and K. Kanie, "Ambient Aqueous-Phase Synthesis of Copper Nanoparticles and Nanopastes with Low-Temperature Sintering and Ultra-High Bonding Abilities," *Sci. Rep.*, vol. 9, pp. 899, 2019.

[4] D. Li, W.-Y. Lai, Y.-Z. Zhang and W. Huang, "Printable Transparent Conductive Films for Flexible Electronics," *Adv. Mater.*, vol. 30, no. 10, pp. 1704738, 2018.

[5] Y. Khan, A. Thielens, S. Muin, J. Ting, C. Baumbauer and A. C. Arias, "A New Frontier of Printed Electronics: Flexible Hybrid Electronics," *Adv. Mater.* vol. 32, no. 15, pp. 1905279, 2020.

[6] T. Minami, "Present status of transparent conducting oxide

thin-film development for Indium-Tin-Oxide (ITO) substitutes," *Thin Solid Films*, vol. 516, no. 17, pp. 5822–5828, 2008.

[7] M. Hwang, B. Jeong, J. Moon, S. Chun and J. Kim, "Inkjet-printing of indium tin oxide (ITO) films for transparent conducting Electrodes," *Mater. Sci. Eng. B*, vol. 176, no. 14, pp. 1128–1131, 2011.

[8] D. Angmo, T. T. Larsen-Olsen, M. Jørgensen, R. R. Søndergaard and F. C. Krebs, "Roll-to-Roll Inkjet Printing and Photonic Sintering of Electrodes for ITO Free Polymer Solar Cell Modules and Facile Product Integration," *Adv. Ener. Mater.*, vol. 3, no. 2, pp. 172–175, 2013.

[9] E. N. Dattoli and W. Lu, "ITO nanowires and nanoparticles for transparent films," *MRS Bull.*, vol. 36, no. 10, pp. 782–788, 2011.

[10] J. Jeong and H. Kim, "Ag nanowire percolating network embedded in indium tin oxide nanoparticles for printable transparent conducting electrodes," *Appl. Phys. Lett.*, vol. 104, pp. 071906, 2014.

[11] H. Shin, K. Kim, T. Kim and H. Kim, "Fiber laser annealing of brush-painted ITO nanoparticles for use as transparent anode for organic solar cells," *Ceram. Int.*, vol. 42, no. 12, pp. 13983–13989, 2016.

[12] T. Kawaharamura, G. T. Dang and M. Furuta, "Successful Growth of Conductive Highly Crystalline Sn-Doped α-Ga$_2$O$_3$ Thin Films by Fine-Channel Mist Chemical Vapor Deposition," *Jpn. Appl. Phys.*, vol. 51, pp. 040207, 2012.

[13] T. Kawaharamura, "Physics on development of open-air atmospheric pressure thin film fabrication technique using mist droplets: Control of precursor flow," *Jpn. Appl. Phys.*, vol. 53, pp. 05FF08, 2014.

[14] T. Shirahata, T. Kawaharamura, S. Fujita and H. Orita, "Transparent conductive zinc-oxide-based films grown at low temperature by mist chemical vapor deposition," *Thin Solid Films*, vol. 597, pp. 30–38, 2015.

[15] G. Qin and A. Watanabe, "Surface Texturing of TiO$_2$ Film by Mist Deposition of TiO$_2$ Nanoparticles," *Nano-Micro Lett.*, vol. 5, no. 2, pp. 129–134, 2013.

[16] R. Suzuki, Y. Nishi, M. Matsubara, A. Muramatsu and K. Kanie, "Single-Crystalline Protrusion-Rich Indium Tin Oxide Nanoparticles with Colloidal Stability in Water for Use in Sustainable Coatings," *ACS Appl. Nano Mater.*, vol. 3, no. 5, pp. 4870–4879, 2020.

[17] K. Kanie, T. Sasaki, M. Nakaya and A. Muramatsu, "Quaternary Ammonium Hydroxides-Assisted Solvothermal Synthesis of Monodispersed ITO Nanoparticles with a Cubic Shape," *Chem. Lett.*, vol. 42, no. 7, pp. 738–740, 2013.

[18] W. Tang, Y. Chao, X. Weng, L. Deng and K. Xu, "Optical Property and the Relationship between Resistivity and Surface Roughness of Indium Tin Oxide Thin Films," *Phys. Procedia*, vol. 32, pp. 680–686, 2012.

鈴木涼子　Ryoko SUZUKI
先進技術開発本部 材料・要素技術研究所
Materials & Advanced Research Laboratory
Advanced Technology Research & Development Division
東北大学
Tohoku University

西　康孝　Yasutaka NISHI
東北大学
Tohoku University
FPD 装置事業部 開発統括部 先端技術開発部
Advanced Technology Development Department
Development Sector
FPD Lithography Business Unit

松原正樹　Masaki MATSUBARA
東北大学
Tohoku University

村松淳司　Atsushi MURAMATSU
東北大学
Tohoku University

蟹江澄志　Kiyoshi KANIE
東北大学
Tohoku University

鈴木涼子
Ryoko SUZUKI

西　康孝
Yasutaka NISHI

松原正樹
Masaki MATSUBARA

村松淳司
Atsushi MURAMATSU

蟹江澄志
Kiyoshi KANIE